Original Article
Food Science and Technology
ISSN 0101-2061 (Print)
ISSN 1678-457X (Online)
DOI: https://doi.org/10.5327/fst.17523
CC BY

Optimizing reaction condition of octenyl succinic anhydride on heat-moisture-treated sago starch and its application for biodegradable film

Angela Myrra Puspita DEWI[1,2], Umar SANTOSO[1], Yudi PRANOTO[1], Djagal Wiseso MARSENO[1*]

Abstract

This study presented the impact of pH and octenyl succinic anhydride (OSA) concentration on the esterification reaction of heat-moisture-treated sago starch (HMT-S) using response surface methodology to achieve optimum degree of substitution (DS), reaction efficiency (RE), and water contact angle (CA). The results showed that HMT-OSA sago starch (HMT-OS) starch exhibited an optimum pH of 7.26 and an OSA concentration of 4.53%. The DS value, RE, and water CA of optimized HMT-OS starch were 0.0121, 33.07%, and 90.11°, respectively. Furthermore, the optimized HMT-OS was used to evaluate the effect of starch modification on film characteristics. HMT-OS film has the best moisture-proof and mechanical properties compared to control (NS), HMT-S, and N-OS films, as indicated by lower water vapor permeability (28.69 g H_2O.mm/s.m^2.Pa × 10^{-11}), water solubility (26.61%), higher CA (104.40°), elongation at break (85.63%), and transparency (3.25% mm^{-1}). According to the scanning electron micrographic images, the absence of cracks or pores was attributed to the waterproof properties and flexibility of the film. Conversely, x-ray diffraction results showed that the crystallinity of HMT-OS film decreased to 36.05%.

Keywords: sago starch; heat-moisture-treated; octenyl succinic anhydride; biodegradable film.

Practical application: This study provides information on optimizing OSA esterification conditions on HMT-S and its application as a material to produce waterproof and stretchable biodegradable films.

1 INTRODUCTION

The current surge of interest in edible and biodegradable films presents an opportunity to replace traditional packaging in a variety of applications. Rong et al. (2023) reported that gallic acid, yam starch, and chitosan films have potential practical applications in pork preservation due to their excellent mechanical, antibacterial, oxidation resistance, and easy degradation properties that can reduce environmental pollution. As an essential biopolymer for the industry, starch is favored for its low cost, abundance, renewability, and degradability (Li et al., 2015). Starches with high amylose content (about 30%) are particularly attractive due to their superior film-forming properties compared to those with low amylose concentration (Bae et al., 2008; Fu et al., 2018). Sago starch, with an amylose content ranging from 27 to 35%, was considered suitable for use as a raw material for producing biodegradable films (Polnaya et al., 2012). However, starch-based films are often characterized by strong hydrophilic properties, brittleness, and a lack of mechanical strength (Majzoobi et al., 2015; Zavareze & Dias, 2011). The two methods used to enhance their water resistance are incorporating hydrophobic substances and hydrophobization of starch.

Esterification using octenyl succinic anhydride (OSA) is a commonly used method for modifying starch to make it more hydrophobic than its native form (Sweedman et al., 2013). The Food and Drug Administration (FDA) has authorized modified starch with OSA as a food ingredient (Bhosale & Singhal, 2006). A previous study showed that sweet potato, sago, corn, and waxy corn starch modified with OSA produced water-resistant and stretchable films (Li et al., 2015; Naseri et al., 2019; Pérez-Gallardo et al., 2012; Zhou et al., 2009). The magnitude of this rise varies depending on the degree of substitution (DS) of OSA starch. Abiddin et al. (2015) investigated several reaction parameters, including OSA concentration, pH, and reaction time, to determine the optimal conditions for producing OS starch with a high DS and reaction efficiency (RE). Recently, several attempts have been conducted to increase the reaction of starch molecules and OSA by removing the tightly packed starch granules, reducing crystallinity, and increasing surface area through physical modification (Chen et al., 2014; Lv et al., 2018).

Heat-moisture treatment is a cost-effective and eco-friendly physical modification method commonly used for food products. Jiranuntakul et al. (2014) have stated that before OSA modification, this treatment could improve DS and RE by facilitating the penetration of OSA into starch granules. Previous studies reported that HMT with a 25% moisture content treatment before esterification of sago starch had the highest DS value and RE of 0.0086 and 35.86%, respectively.

Heat-moisture treatment before OSA modification could minimize the esterification reaction conditions to obtain high DS, RE, and starch hydrophobicity. However, the optimization of the OSA esterification reaction on HMT-sago starch (HMT-S)

Received 7 Mar., 2023
Accepted 23 May, 2023
[1]*Gadjah Mada University, Faculty of Agricultural Technology, Department of Food and Agricultural Product Technology, Sleman, Yogyakarta, Indonesia.*
[2]*Papua University, Faculty of Agricultural Technology, Department of Agricultural Technology, Manokwari, West Papua, Indonesia.*
*Corresponding author: djagal@ugm.ac.id

and the application of HMT-OSA sago starch (HMT-OS) as a raw material to produce a biodegradable film have not been studied. Therefore, this study aimed to obtain the optimum conditions for preparing HMT-OS using response surface methodology (RSM) by evaluating DS, RE, hydrophobicity, mechanical properties, and a moisture-proof biodegradable film.

2 MATERIALS AND METHODS

2.1 Materials

Sago starch (*Metroxylon* sp.) was purchased from a domestic shop in Manokwari, Indonesia. OSA reagent and glycerol were acquired from Sigma-Aldrich Corporation.

2.2 Methods

2.2.1. Heat-moisture-treated sago starch

HMT-S was prepared based on the method described by Dewi et al. (2022) and Pukkahuta and Varavinit (2007). Sago starch was sprayed with the specified amount of distilled water before being homogenized for 20 min to obtain a 25% moisture content. A moisture analyzer (MB120, Ohaus, Shanghai, China) was used to determine the actual moisture content of the combination. After an hour of incubation, HMT-S was put in a 500-mL Duran glass with a screw top and autoclaved. The bottles were heated for 1 h at 120 °C, then dried in a cabinet dryer at 50 °C after being allowed to cool to room temperature. Finally, HMT-S was employed to optimize the octenyl succinate modification.

2.2.2 Preparation of HMT-OS

The procedure of Jiranuntakul et al. (2014) was followed in the preparation of OSA. HMT-S was dispersed in distilled water (30% w/v). The pH of the slurry was controlled from 5 to 9 using a pH meter by adding a 3% NaOH solution. Subsequently, OSA reagent of 3–7% (based on dry starch basis) was gradually added over 2 h (five times diluted with isopropyl alcohol, v/v) while preserving the pH and steady stirring. Esterification was conducted for 4 h at 35 °C, and the pH was adjusted to 6.5 at the end of the reaction using a 3% HCl solution. Finally, HMT-OS starches were collected using a vacuum filter, washed twice with distilled water and twice with 70% aqueous alcohol, and dried at 40 °C for 24 h.

2.2.3 Experimental design

The effect of the independent variables, namely pH (X1) and OSA concentration (X2), on DS, RE, and water contact angel (CA) was calculated using RSM. The response surface design uses independent variables, and their levels were coded as -α -1, 0, +1, and +α (α=1.414), as shown in Table 1.

Table 1. Independent variables and factor levels used in the RSM.

Independent variables	Factor level				
	-α	-1	0	+1	+α
pH	4.17	5	7	9	9.83
OSA concentration (%)	2.17	3	5	7	7.83

Experiments were designed using a central composite design (CCD), which consists of 13 experimental runs and 5 center-point replicates. Design-Expert 13.0 (Stat-Ease Inc., Minneapolis) was used to analyze the model that best fits the response conditions. After receiving the optimization results, they were validated to determine the accuracy of their model, and this was conducted by comparing the predicted optimal and the actual results. Finally, the outcomes of the comparison are processed using linear regression plots.

2.2.4 DS value and RE of HMT-OS

DS and RE were obtained by alkali saponification, followed by titrimetric reverse titration of any excess alkali (Bhosale & Singhal, 2006). RE was determined using Equation 1:

$$RE = \frac{\text{actual DS}}{\text{Theoretical DS}} \times 100\% \quad (1)$$

Theoretical DS was calculated by assuming that all the added OSA interacted with the starch to generate the ester derivative.

2.2.5 Water CA of starches and biodegradable films

Water CA was measured with a custom-built optical sessile drop device integrated with a USB Digital Microscope (Herniou-Julien et al., 2019; Piñeros-Hernandez et al., 2017). The starch samples were prepared and analyzed following the procedures of Dewi et al. (2022), which were applied to the surface of biodegradable film, and the drop image was captured using a digital microscope. Furthermore, the water CA was examined using the ImageJ software, and the reported value is the mean of at least five separate measurements.

2.2.6 Fourier transform infrared spectra

An FTIR spectrophotometer (FTIR Thermo Nicolet IS 10, Thermo Fischer Scientific, Madison, WI, USA) was used to determine the spectra of native and modified starches. The samples were dried and crushed with KBr at a ratio of 1:100 (w/w). Finally, the resulting mixture was scanned over the 400–4,000 cm^{-1} wavenumber range with 8 cm^{-1} resolution.

2.2.7 ^{1}H NMR and ^{13}C NMR spectra

^{1}H NMR and ^{13}C NMR analyses were conducted by spectrometer JEOL JNM-ECZR 500 MHz instrument (JNM-ECZ500R/S1, IOCB, Prague), where starch dissolution was mixed with 600 µL of DMSO-d6, following the procedure outlined by Q. Wang et al. (2022). Data collection for the ^{1}H NMR spectrum was maintained at 23.2 °C for 64 scans and 4,096 scans for the ^{13}C NMR spectrum. The acquisition time and relaxation delay were 0.83 and 2.0 s, respectively. Finally, the collected data were processed by the MestReNova software (MNova 14.0, MestreLab Research, Spain).

2.2.8 Preparation of biodegradable film

Starch films have been produced by casting 3.0% native and modified starch suspensions using glycerol as the plasticizer (0.30 g/g of starch). The film-forming suspension was heated

for 30 min at 90 °C with constant agitation, as described by Li et al. (2015). The solutions were poured onto polyethylene plates (10 × 15 cm) and dried at 40 °C for 24 h in an oven with circulating air. Finally, the dried samples were conditioned at RH 56%, 72 h before analysis.

2.2.9 Water solubility and water vapor permeability of film measurement

The solubility was determined by calculating the percentage of solubilized film dry mass after 24 h of immersion in 30 °C water, following Gontard et al. (1994). WVP tests were conducted using the E96-95 ASTM standard method (Bertuzzi et al., 2007).

2.2.10 Mechanical properties of films

Tensile strength and elongation of each film were analyzed according to ASTM-D D412-98a (ASTM, 1998) using a Universal Testing Machine (Zwick Z0.5, West Sussex) with a velocity of 1.0 mm s^{-1} and a 50 mm distance between clamps. Test samples were cut in dumbbell die "I" dimensions (Dumb Bell Ltd., Saitana, Japan) as specified by the ASTM standard method. The results are the average of three samples.

2.2.11 Films characterization

Film samples were characterized by x-ray diffraction (XRD) and scanning electron microscopy (SEM). The XRD were acquired using a diffractometer (Rigaku-Nex QC+QuanTEZ, Applied Rigaku Technologies, Inc., Austin, USA) with Cu Kα radiation (λ=0.154 nm) at 30 °C, and the scanning range of the diffraction angle (2θ) was from 4° to 40°. Furthermore, the collected data were processed using the Origin Pro software (OriginPro 2019, OriginLab Corporation, Northampton, MA, USA).

Micrographs of the surface and cross-sections of the films were obtained using SEM (JSM-6510LA, JEOL, Akishima, Tokyo, Japan). The specimens were cryofractured by immersion in liquid nitrogen. Subsequently, a voltage of roughly 10 kV was used to acquire images at various magnifications of 1,000× to 10,000×.

3 RESULTS AND DISCUSSION

3.1 Effect of pH and concentration OSA on DS, RE, and water CA

A CCD experimental design was used to investigate the effect of the independent variables on DS, RE, and CA. The results were analyzed using analysis of variance (ANOVA) to evaluate the model's accuracy, as shown in Table 2. The response variable is considered significant when the p-value for each term is less than 0.05 ($p<0.05$). The coefficient of determination (R^2) ranged from 0.9806 to 0.9813, which indicated that 98% of the variance was due to pH and OSA concentration. According to the ANOVA results, the quadratic models of DS, RE, and CA were significant ($p<0.05$). The adjusted value of determination (R^2 adj 0.9668–0.9831), which is close to R^2 (the difference <0.2), confirmed the high significance of the inferred model. A lack of fit (LOF) test was conducted to determine the model's acceptability. The ANOVA test of the DS response shows the LOF test is significant ($p<0.05$), indicating that the model cannot be utilized to predict optimization. Meanwhile, the LOF values of RE and CA are insignificant ($p>0.05$), indicating that the model is acceptable for predicting optimization conditions. A nonsignificant LOF value ($p>0.05$) suggests that the response data are compatible with the model (Rai Widarta et al., 2022).

The 3D response surface plot in Figure 1 shows DS value, RE, and CA as a function of pH (X1) and OSA concentration (X2). A higher concentration of OSA increased DS, which was decreased by a higher pH. This condition elevates RE to 5% and flattens until 7% OSA concentration. The same phenomenon has also been reported in sweet potato (Lv et al., 2018; Shi & He, 2012) and pearl millet starch (Sharma et al., 2016). Excessive OSA concentration decreases RE due to steric inhibition that restricts the accessibility of starch molecules and avoids the reaction process (Lv et al., 2018). Furthermore, the decrease in RE is also due to insufficient mixing between the water-insoluble OSA and the starch phase (Shi & He, 2012). According to the 3D response surface plot (Figure 1C), increasing the reaction pH and OSA concentration to a particular level elevated the water CA due to the hydroxyl groups on starch molecules being replaced by lipophilic octenyl groups through esterification (Dewi et al., 2022; Sweedman et al., 2013). The reaction pH conditions and OSA concentration lead to a decrease in the water CA. This is because anhydride hydrolysis occurs and facilitates de-esterification (Bhosale & Singhal, 2006; Hui et al., 2009; Segura-Campos et al., 2008).

3.2 Optimization and validation experiment

In this dual HMT-OS, this study aimed to obtain the maximum RE and CA values of starch. The effect of each variable was predicted using the Design-Expert software. The optimum pH and OSA concentration reaction conditions were 7.27 and 4.53%, respectively, with predicted DS 0.013, RE 33.61%, and CA 90.67°. Furthermore, the desirability value was 0.96. The predicted values of DS, RE, and CA can be validated by conducting

Table 2. Estimated regression coefficient and ANOVA for DS, RE, and CA.

Term	Estimated regression coefficient					
	Degree of substitution	p-value	Reaction efficiency	p-value	Contact angle	p-value
Model		<0.0001		<0.0001		<0.0001
Lack of fit		0.0089		0.0599		0.1314
R^2	0.9814		0.9831		0.9806	
R^2 adj	0.9679		0.9710		0.9668	
R^2 prediction	0.8739		0.8970		0.8923	

verification experiments under optimum conditions. Three replications of confirmation experiments were performed, and the optimal parameters were validated using the T-test. The average values obtained from the actual studies were DS 0.0121±0.00, RE 33.07%±0.21, and CA 90.11°±0.88. The results showed no significant difference between the actual and predicted values, implying that the obtained figures agreed with those calculated by the software. This value of DS is similar to the previous study, but the optimal OSA concentration is lower than that reported by Abiddin et al. (2015). Additionally, this study's reaction time was faster than the previous report, indicating that the esterification reaction between OSA groups and starch molecules was more efficient. HMT pretreatment facilitates the entry of OSA into starch granules and enhances its reaction with hydroxyl groups (Jiranuntakul et al., 2014; Lv et al., 2018). Finally, it increases the amorphous area and changes the crystal organization, resulting in more available sites for the reaction (Dewi et al., 2022).

3.3 Identification and prediction of HMT-OSA starch molecular structure

Figure 2 shows the FT-IR spectra of native sago starch (NS), HMT sago starch (HMT-S), OSA-sago starch (N-OS), HMT-OSA sago starch (HMT-OS), and commercial OSA starch. There were similar absorption bands in all five spectra, including at 3,420 cm^{-1} (O-H) and 2,924 cm^{-1} (C-H), while 1,640 cm^{-1} was associated with residual bound water. The C-O stretching vibration of the anhydrous-glucose unit has detectable adsorption bands at 1,159, 1,082, and 1,019 cm^{-1} (Naseri et al., 2019). There were new absorption peaks at 1,579 and 1,726 cm^{-1} in N-OS and HMT-OS, which were attributed to asymmetric carboxylate ($RCOO^-$) and C=O stretching vibrations of the carbonyl ester group, respectively (Dewi et al., 2022; Sharma et al., 2016; Zhang et al., 2021). These were also detected in commercial OSA starch, as presented in Figure 2C. The two additional peaks confirm that the hydroxyl group in the starch molecule has been substituted with the ester carbonyls and the carboxyl group of OSA (Zainal Abiddin et al., 2018). Compared to OSA-modified sago starch (N-OS), the intensity of the absorption peaks at wavelengths of 1,579 and 1,726 cm^{-1} of HMT-OS is higher because DS (0.0121±0.0008) is greater than that of N-OS (0.0069±0.0009) (Sun et al., 2020; Zhang et al., 2013).

The investigation of the molecular structure of HMT-OS was conducted using ^1H and ^{13}C NMR, and the corresponding spectra are displayed in Figure 3A and 3B. Figure 3A indicates that the ^1H spectra of NS and HMT-S appear to have no difference, but there is a decrease in intensity at 4.98 ppm in the spectrum. The reduction in the intensity of the resonance peak can be attributed to the α-(1, 6)-glycosidic bond being more severely damaged than the α-(1, 4)-glycosidic due to the weak steric hindrance (Acevedo et al., 2022; Wang et al., 2022). HMT-OS spectra showed a new peak at 0.80–2.7 ppm, which is associated with OSA esterification of the starch molecule (Simsek et al., 2015; Tong et al., 2019). Additional resonances in HMT-OS were also detected at 0.82 ppm (the terminal H methyl proton), 1.23 ppm (H8–H10), and 1.90–2.20 (H11, H14–H16) (Bai et al., 2011; Wang et al., 2020).

The ^{13}C chemical shifts of glucose residues were obtained from the ^{13}C NMR spectrum of native starch (Figure 3B). The peaks in the C1 region are typical characteristics of V-type single helices (eight glucose cycles per round), while those around C4 are amorphous crossing points associated with the amylopectin double helix (Liu et al., 2019; Sudlapa & Suwannaporn, 2023;

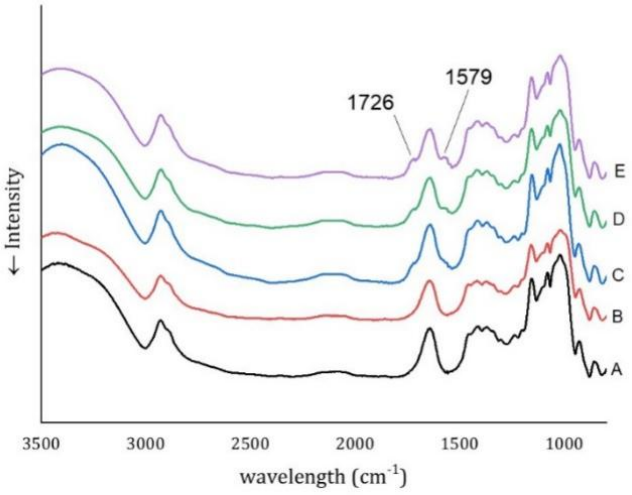

Figure 2. (A) FT-IR spectra of native sago starch, (B) HMT sago starch, (C) OSA commercial starch, (D) OSA-sago starch, and (E) HMT-OSA sago starch.

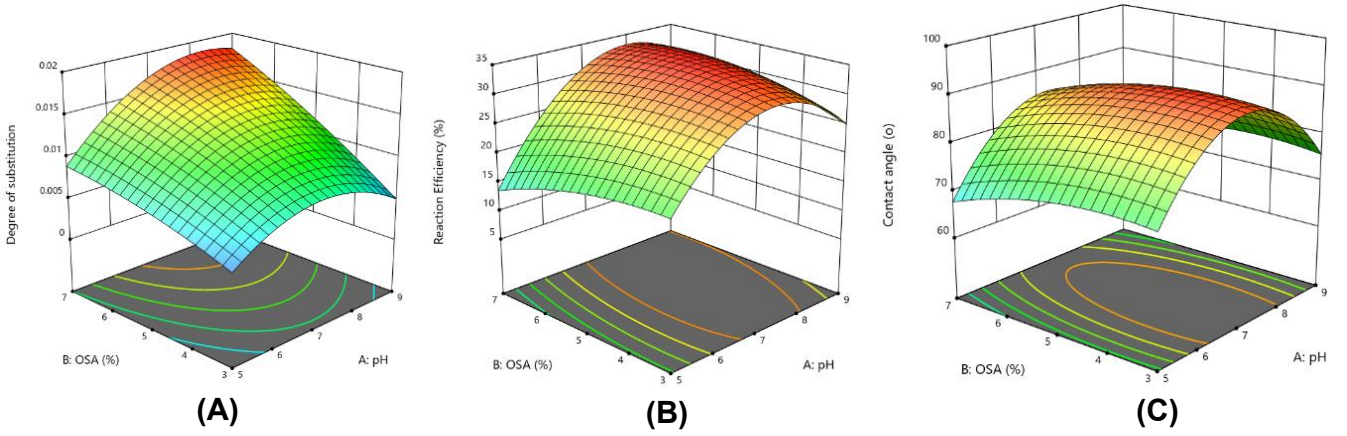

Figure 1. (A) Plot 3D surface response of degree of substitution, (B) reaction efficiency, and (C) water contact angle.

Xie et al., 2020). HMT decreases the percentage of double helices and increases single helices, resulting in a higher moisture content treatment and reduced relative crystallinity (Du et al., 2023; Wang et al., 2018).

The OSA group has been successfully incorporated into the starch molecule, as confirmed by the appearance of new resonances corresponding to those of the OSA reagent at 14.54 ppm for C7, 22.48 ppm for C8, and 28.55–31.82 ppm for C9–C11. The location of the substitution reaction can be determined from ^{13}C NMR spectroscopy (Gao et al., 2021). Based on Figure 3B, the C1 signal of HMT-OS becomes broader than HMT (Figure 3B), confirming that OSA substitution occurs at OH-2 (Bai et al., 2011; Zhang et al., 2013). Furthermore, a broadened peak was observed at 79 ppm resonance and a new 72 ppm resonance, indicating that the OSA group was substituted at the OH-3 position in HMT-OS, as reported by Gao et al. (2021). Therefore, OSA substitution occurs at OH-2 and OH-3 of the glucose residues in HMT-S.

3.4 Characteristics of biodegradable film

3.4.1 WVP, water CA, and water solubility of films

The hydrophobic properties of the films from HMT-OS were discovered to be the best, as they exhibited the lowest WVP and solubility values and the highest CA when compared to all film samples, as shown in Table 3. HMT before OSA esterification caused more OSA groups to penetrate the internal starch granules, which is consistent with the DS value data. The hydrophobicity of the film surface was assessed using the sessile drop procedure, which measured the water CA (θ) on the film surface. In general, larger values imply greater surface hydrophobicity, and the quantitative distinction between "hydrophobic" and "hydrophilic" surfaces is based on when θ>65 or θ<65, respectively (Piñeros-Hernandez et al., 2017). The water CA value of OSA films was >95°, indicating that the esterification increased hydrophobicity. HMT pretreatment before OSA produced films with the highest water CA, which agrees with WVP and solubility data. The increase in CA in modified starch films is attributed to surface polarity due to the introduction of hydrophobic octenyl groups (Naseri et al., 2019).

The solubility of NS, N-OS, HMT-S, and HMT-OS films is presented in Table 3. Higher values typically indicate lower water resistance, and the solubility of HMT-S film is lower than that of NS. This is consistent with the results reported in the film made from sweet potato starch (Indrianti et al., 2018), chestnut starch (Singh et al., 2009), rice starch (Majzoobi et al., 2015), and waxy corn starch (Pérez-Gallardo et al., 2012). The decrease in water solubility of HMT-S is related to the strengthening of intermolecular bonds promoted by HMT, thereby reducing water absorption capacity (Huang et al., 2016). It was stated that the solubility of N-OS and HMT-OS films decreased by 21.78 and 42.77%, respectively. Li et al. (2015) reported that increasing the hydrophobic properties of starch films through esterification reduces the availability of hydroxyl groups and inhibits water access into the matrix, thereby decreasing the film's solubility along with increasing its DS value.

3.4.2 Mechanical and transparency of starch films

The mechanical properties and chemical structure of film materials are often described by their tensile strength and elongation at break (EAB), while the transparency of starch films plays a crucial role in their usage as surface coatings for packaged

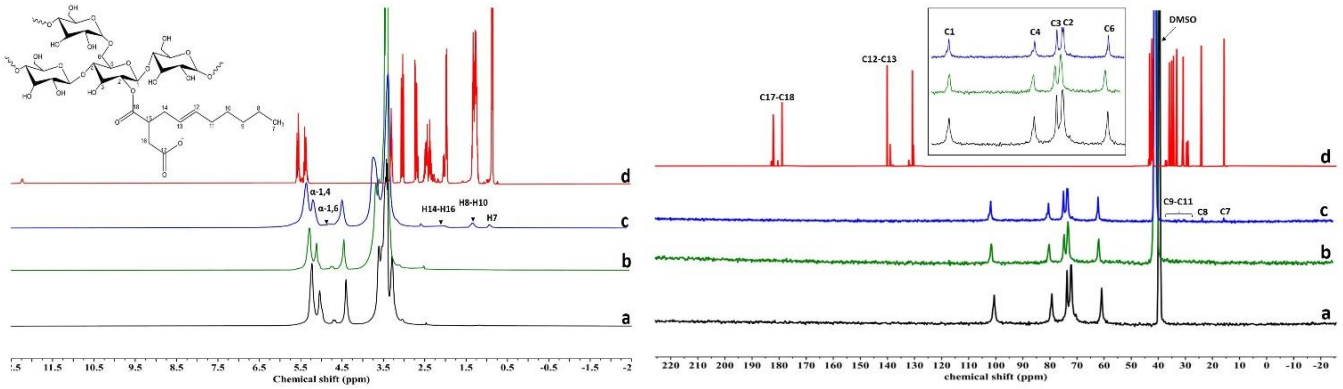

Figure 3. (A) ^{1}H-NMR and (B) ^{13}C-NMR spectra of (a) native sago starch, (b) HMT-S, (c) HMT-OS, and (d) OSA reagent.

Table 3. Properties of starch films prepared from native, heat-moisture-treated octenyl succinate and HMT-OS.

Sample	WVP (g.mm/s.m^2.Pa)×10^{-11}	CA (°)	Water Solubility (%)	TS (MPa)	Elongation at break (%)	Transparency (%mm^{-1})
NS	46.96±4.65^{ab}	39.10±2.82^{c}	46.50±3.50^{a}	1.22±0.25^{a}	33.52±0.95^{c}	3.13±0.04^{b}
N-OS	42.30±2.06^{b}	95.32±3.27^{b}	36.37±2.72^{b}	0.87±0.36^{ab}	74.60±5.29^{b}	3.26±0.06^{a}
HMT-S	53.80±3.68^{a}	39.52±3.01^{c}	31.89±4.19^{bc}	1.32±0.32^{a}	17.70±1.78^{c}	3.11±0.06^{b}
HMT-OS	28.69±3.44^{c}	104.40±2.02^{a}	26.61±6.83^{c}	0.66±0.03^{b}	85.63±1.25^{a}	3.25±0.05^{a}

Means with different superscript letters within a column are significantly different (p≤0.05). NS: native sago starch; HMT-S: HMT sago starch; N-OS: OSA-sago starch; HMT-OS: HMT-OSA sago starch.

foods. The high intensity of intermolecular interactions between polymer chains in the film matrix enhances tensile strength while decreasing EAB. Notably, the EAB values of OSA starch films were observed to be higher than those of NS films, confirming that OSA enhanced stretchability (Li et al., 2015; Naseri et al., 2019). HMT-OS films were found to provide higher EAB values than N-OS films, which can be attributed to the DS value (Li et al., 2015; Li et al., 2018). The octenyl groups in modified starch act like plasticizers by preventing the formation of hydrogen bonds and van der Waals forces between adjacent polymer chains, thereby increasing their mobility (Naseri et al., 2019).

Transparent films are characterized by high transparency values (Majzoobi et al., 2015). The transparency of OSA films was more elevated than that of SS films. However, there was no significant difference in the transparency of N-OS and HMT-OS films. Naseri et al. (2019) reported that OSA modification reduced the turbidity of sago starch films due to the disruption of the structural order, which increased light transmission. Finally, octenyl succinate polysaccharides were shown to form ordered self-aggregates in aqueous media, reducing light absorbance and consequently increasing film transparency (Li et al., 2015).

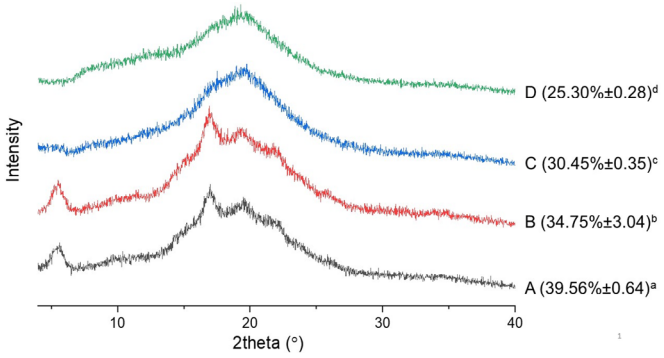

Figure 4. XRD and relative crystallinity of (A) native sago starch, (B) HMT-S, (C) N-OS, and (D) HMT-OS films.

3.4.3 XRD and crystallinity of films

XRD of sago starch films is characteristic of type C starch, as noted in previous studies (Dewi et al., 2022; Naseri et al., 2019; Pukkahuta & Varavinit, 2007; Santoso et al., 2021). Based on Figure 4, there was no alteration in the diffraction-type pattern of HMT-S films. However, no clear diffraction peaks were observed for N-OS and HMT-OS films, indicating that they have much lower crystallinity than the control films. As observed in this study, the incorporation of OS groups was found to lower the crystallinity formation ability of starch molecules, as reported by Li et al. (2015), Naseri et al. (2019), and Zhou et al. (2009). This is due to the steric hindrance of OSA groups on starch chain compaction via hydrogen bonding during the film formation process, resulting in a reduction of the crystallinity of the films. The low RC value of HMT-OS film (25.30%) is related to its low tensile strength. Indrianti and Pranoto (2018) stated that the film's crystallinity affected the structure's compactness.

3.4.4 Morphology of biodegradable film

Figure 5 shows micrographs of biodegradable films used to evaluate their surface structure and transverse perspective. The HMT film surface is smoother than the surface of the control. Viana et al. (2022) reported that bioplastics from HMT banana starch produced homogeneous and well-structured surfaces attributed to the rearrangement and interaction of amylose and amylopectin molecules in the film-form matrix. In terms of the cross-sectional appearance of the control film (NS) and HMT-S, some cracks were attributed to the hydrophilicity of native and HMT-S as well as the low EAB value. In contrast, N-OS and HMT-OS starch film micrographs showed a transverse perspective without cracks or pores. Panrong et al. (2020) discovered that LLDPE/OS blend films are less hydrophilic and have fewer pores. The absence of cracks or pores in OSA starch film is related to its waterproof properties and flexibility.

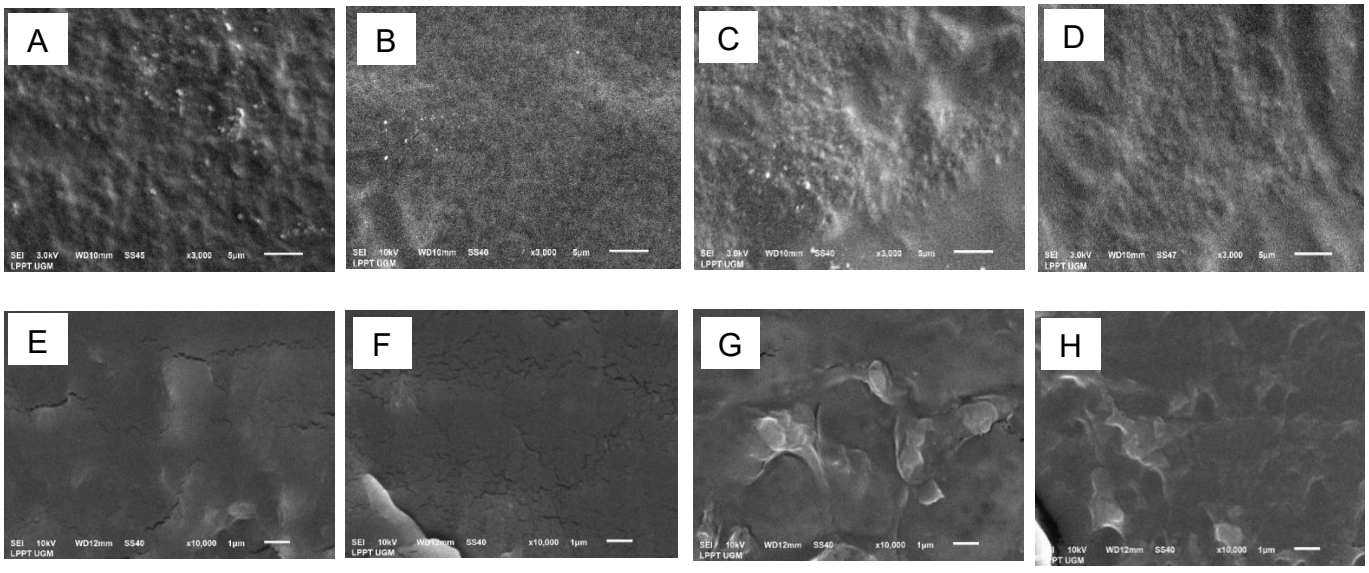

Figure 5. (A, B, C, D) SEM images of surface and (E, F, G, H) cross-section of (A and E) native sago starch, (B and F) HMT-S, (C and G) N-OSA starch, and (D and H) HMT-OSA starch films.

4 CONCLUSION

HMT sago starch was successfully esterified with OSA, and the main factors affecting the modification were investigated. All variables studied were proven to affect RE and CA. Based on the results, the optimum conditions for RE and CA were pH and OSA concentrations of 7.27 and 4.53%, respectively. The esterification of HMT-S at optimum conditions was proven to increase hydrophobicity and was successfully applied to improve the waterproof properties of biodegradable films. Furthermore, HMT-OS starch biodegradable film has better water resistance and stretchability properties. WVP and water solubility of HMT-OS film decreased by 38.91 and 42.77%, respectively. Meanwhile, the film's water CA and EAB increased by 167 and 155.46%, respectively, and it also has good transparency.

ACKNOWLEDGMENTS

The authors would like to express their appreciation to the Indonesian Endowment Fund for Education (LPDP Indonesia) and the Ministry of Finance of the Republic of Indonesia No: KET-1474/LPDP.4/2019.

REFERENCES

Abiddin, Z., Yusoff, A., & Ahmad, N. (2015). Optimisation of reaction conditions of octenyl succinic anhydride (OSA) modified sago starch using response surface methodology (RSM). *Internationa; Food Research Journal*, *22*(3), 930-935.

Acevedo, B. A., Villanueva, M., Chaves, M. G., Avanza, M. V., & Ronda, F. (2022). Modification of structural and physicochemical properties of cowpea (Vigna unguiculata) starch by hydrothermal and ultrasound treatments. *Food Hydrocolloids*, *124*(Part A), 107266. https://doi.org/10.1016/j.foodhyd.2021.107266

American Society for Testing and Materials (ASTM) (1998). *AST-MD412-98a*. Standard Test Methods for vulcanized rubber and thermoplastic elastomers-tension Annual book of ASTM standards. ASTM.

Bae, H. J., Cha, D. S., Whiteside, W. S., & Park, H. J. (2008). Film and pharmaceutical hard capsule formation properties of mungbean, waterchestnut, and sweet potato starches. *Food Chemistry*, *106*(1), 96-105. https://doi.org/10.1016/j.foodchem.2007.05.070

Bai, Y., Shi, Y. C., Herrera, A., & Prakash, O. (2011). Study of octenyl succinic anhydride-modified waxy maize starch by nuclear magnetic resonance spectroscopy. *Carbohydrate Polymers*, *83*(2), 407-413. https://doi.org/10.1016/j.carbpol.2010.07.053

Bertuzzi, M. A., Castro Vidaurre, E. F., Armada, M., & Gottifredi, J. C. (2007). Water vapor permeability of edible starch based films. *Journal of Food Engineering*, *80*(3), 972-978. https://doi.org/10.1016/j.jfoodeng.2006.07.016

Bhosale, R., & Singhal, R. (2006). Process optimization for the synthesis of octenyl succinyl derivative of waxy corn and amaranth starches. *Carbohydrate Polymers*, *66*(4), 521-527. https://doi.org/10.1016/j.carbpol.2006.04.007

Chen, X., He, X., & Huang, Q. (2014). Effects of hydrothermal pretreatment on subsequent octenylsuccinic anhydride (OSA) modification of cornstarch. *Carbohydrate Polymers*, *101*, 493-498. https://doi.org/10.1016/j.carbpol.2013.09.079

Dewi, A. M. P., Santoso, U., Pranoto, Y., & Marseno, D. W. (2022). Dual Modification of Sago Starch via Heat Moisture Treatment and Octenyl Succinylation to Improve Starch Hydrophobicity. *Polymers*, *14*(6), 1086. https://doi.org/10.3390/polym14061086

Du, M., Cao, T., Yu, M., Zhang, C., & Xu, W. (2023). Effect of heat-moisture treatment on physicochemical properties of chickpea starch. *Food Science and Technology*, *43*, e108822. https://doi.org/10.1590/fst.108822

Fu, L., Zhu, J., Zhang, S., Li, X., Zhang, B., Pu, H., Li, L., & Wang, Q. (2018). Hierarchical structure and thermal behavior of hydrophobic starch-based films with different amylose contents. *Carbohydrate Polymers*, *181*, 528-535. https://doi.org/10.1016/j.carbpol.2017.12.010

Gao, W., Liu, P., Wang, B., Kang, X., Zhu, J., Cui, B., & El-, A. M. A. (2021). Synthesis, physicochemical and emulsifying properties of C-3 octenyl succinic anhydride-modified corn starch. *Food Hydrocolloids*, *120*, 106961. https://doi.org/10.1016/j.foodhyd.2021.106961

Gontard, N., Duchez, C., Cuq, J.-L., & Guilbert, S. (1994). Edible composite films of wheat gluten and lipids: water vapour permeability and other physical properties. *International Journal of Food Science and Technology*, *29*(1), 39-50. https://doi.org/10.1111/j.1365-2621.1994.tb02045.x

Herniou-Julien, C., Mendieta, J. R., & Gutiérrez, T. J. (2019). Characterization of biodegradable / non-compostable fi lms made from cellulose acetate / corn starch blends processed under reactive extrusion conditions. *Food Hydrocolloids*, *89*, 67-79. https://doi.org/10.1016/j.foodhyd.2018.10.024

Huang, T. T., Zhou, D. N., Jin, Z. Y., Xu, X. M., & Chen, H. Q. (2016). Effect of repeated heat-moisture treatments on digestibility, physicochemical and structural properties of sweet potato starch. *Food Hydrocolloids*, *54*(Part A), 202-210. https://doi.org/10.1016/j.foodhyd.2015.10.002

Hui, R., Qi-he, C., Ming-liang, F., Qiong, X., & Guo-qing, H. (2009). Preparation and properties of octenyl succinic anhydride modified potato starch. *Food Chemistry*, *114*(1), 81-86. https://doi.org/10.1016/j.foodchem.2008.09.019

Indrianti, N., & Pranoto, Y. (2018). Physicochemical properties of modified sweet potato starch through heat moisture treatment. *AIP Conference Proceedings* .

Indrianti, N., Pranoto, Y., & Abbas, A. (2018). Preparation and characterization of edible films made from modified sweet potato starch through heat moisture treatment. *Indonesian Journal of Chemistry*, *18*(4), 679-687. https://doi.org/10.22146/ijc.26740

Jiranuntakul, W., Puncha-arnon, S., & Uttapap, D. (2014). Enhancement of octenyl succinylation of cassava starch by prior modification with heat-moisture treatment. *Starch/Staerke*, *66*(11-12), 1071-1078. https://doi.org/10.1002/star.201400115

Li, J., Ye, F., Lei, L., & Zhao, G. (2018). Combined effects of octenylsuccination and oregano essential oil on sweet potato starch films with an emphasis on water resistance. *International Journal of Biological Macromolecules*, *115*, 547-553. https://doi.org/10.1016/j.ijbiomac.2018.04.093

Li, J., Ye, F., Liu, J., & Zhao, G. (2015). Effects of octenylsuccination on physical, mechanical and moisture-proof properties of stretchable sweet potato starch film. *Food Hydrocolloids*, *46*, 226-232. https://doi.org/10.1016/j.foodhyd.2014.12.017

Liu, K., Zhang, B., Chen, L., Li, X., & Zheng, B. (2019). Hierarchical structure and physicochemical properties of highland barley starch following heat moisture treatment. *Food Chemistry*, *271*, 102-108. https://doi.org/10.1016/j.foodchem.2018.07.193

Lv, Q., Li, G., Xie, Q., Zhang, B., Li, X., Pan, Y., & Chen, H. (2018). Evaluation studies on the combined effect of hydrothermal treatment and octenyl succinylation on the physicochemical, structural and digestibility characteristics of sweet potato starch. *Food Chemistry*, *256*, 413-418. https://doi.org/10.1016/j.foodchem.2018.02.147

Majzoobi, M., Pesaran, Y., Mesbahi, G., & Golmakani, M. T. (2015). Physical properties of biodegradable films from heat-moisture-treated rice flour and rice starch. *Starch / Stärke*, *67*(11-12), 1053-1060. https://doi.org/10.1002/star.201500102

Naseri, A., Shekarchizadeh, H., & Kadivar, M. (2019). Octenylsuccination of sago starch and investigation of the effect of calcium chloride and ferulic acid on physicochemical and functional properties of the modified starch film. *Food Processing and Preservation*, *43*(3), e13898. https://doi.org/10.1111/jfpp.13898

Panrong, T., Karbowiak, T., & Harnkarnsujarit, N. (2020). Effects of acetylated and octenyl-succinated starch on properties and release of green tea compounded starch/LLDPE blend films. *Journal of Food Engineering*, *284*, 110057. https://doi.org/10.1016/j.jfoodeng.2020.110057

Pérez-Gallardo, A., Bello-Pérez, L. A., García-Almendárez, B., Montejano-Gaitán, G., Barbosa-Cánovas, G., & Regalado, C. (2012). Effect of structural characteristics of modified waxy corn starches on rheological properties, film-forming solutions, and on water vapor permeability, solubility, and opacity of films. *Starch/Staerke*, *64*(1), 27-36. https://doi.org/10.1002/star.201100042

Piñeros-Hernandez, D., Medina-Jaramillo, C., López-Córdoba, A., & Goyanes, S. (2017). Edible cassava starch films carrying rosemary antioxidant extracts for potential use as active food packaging. *Food Hydrocolloids*, *63*, 488-495. https://doi.org/10.1016/j.foodhyd.2016.09.034

Polnaya, F., Talahatu, J., Haryadi, & Marseno, D. W. (2012). Properties of biodegradable films from hydroxypropyl sago starches. *Asian Journal of Food and Agro-Industry*, *5*(3), 183-192.

Pukkahuta, C., & Varavinit, S. (2007). Structural transformation of sago starch by heat-moisture and osmotic-pressure treatment. *Starch/Staerke*, *59*(12), 624-631. https://doi.org/10.1002/star.200700637

Rai Widarta, I. W., Rukmini, A., Santoso, U., Supriyadi, & Raharjo, S. (2022). Optimization of oil-in-water emulsion capacity and stability of octenyl succinic anhydride-modified porang glucomannan (*Amorphophallus muelleri* Blume). *Heliyon*, *8*(5), 09523. https://doi.org/10.1016/j.heliyon.2022.e09523

Rong, L., Ji, X., Shen, M., Chen, X., Qi, X., Li, Y., & Xie, J. (2023). Characterization of gallic acid-Chinese yam starch biodegradable film incorporated with chitosan for potential use in pork preservation. *Food Research International*, *164*, 112331. https://doi.org/10.1016/j.foodres.2022.112331

Santoso, B., Sarungallo, Z. L., & Puspita, A. M. (2021). Physicochemical and functional properties of spineless, short-spines, and long-spines sago starch. *Biodiversitas*, *22*(1), 137-143. https://doi.org/10.13057/biodiv/d220119

Segura-Campos, M., Chel-Guerrero, L., & Betancur-Ancona, D. (2008). Synthesis and partial characterization of octenylsuccinic starch from Phaseolus lunatus. *Food Hydrocolloids*, *22*(8), 1467-1474. https://doi.org/10.1016/j.foodhyd.2007.09.009

Sharma, M., Singh, A. K., Yadav, D. N., Arora, S., & Vishwakarma, R. K. (2016). Impact of octenyl succinylation on rheological, pasting, thermal and physicochemical properties of pearl millet (Pennisetum typhoides) starch. *LWT - Food Science and Technology*, *73*, 52-59. https://doi.org/10.1016/j.lwt.2016.05.034

Shi, S. S., & He, G. Q. (2012). Process optimization for cassava starch modified by octenyl succinic anhydride. *Procedia Engineering*, *37*, 255-259. https://doi.org/10.1016/j.proeng.2012.04.236

Simsek, S., Ovando-Martinez, M., Marefati, A., Sj, M., & Rayner, M. (2015). Chemical composition, digestibility and emulsification properties of octenyl succinic esters of various starches. *Food Research International*, *75*, 41-49. https://doi.org/10.1016/j.foodres.2015.05.034

Singh, G. D., Bawa, A. S., Riar, C. S., & Saxena, D. C. (2009). Influence of heat-moisture treatment and acid modifications on physicochemical, rheological, thermal and morphological characteristics of indian water chestnut (trapa natans) starch and its application in biodegradable films. *Starch/Staerke*, *61*(9), 503-513. https://doi.org/10.1002/star.200900129

Sudlapa, P., & Suwannaporn, P. (2023). Dual complexation using heat moisture treatment and pre-gelatinization to enhance Starch – Phenolic complex and control digestibility. *Food Hydrocolloids*, *136*(Part A), 108280. https://doi.org/10.1016/j.foodhyd.2022.108280

Sun, S., Lin, X., Zhao, B., Wang, B., & Guo, Z. (2020). Structural properties of lotus seed starch prepared by octenyl succinic anhydride esterification assisted by high hydrostatic pressure treatment. *LWT - Food Science and Technology*, *117*, 108698. https://doi.org/10.1016/j.lwt.2019.108698

Sweedman, M. C., Tizzotti, M. J., Schäfer, C., & Gilbert, R. G. (2013). Structure and physicochemical properties of octenyl succinic anhydride modified starches: A review. *Carbohydrate Polymers*, *92*(1), 905-920. https://doi.org/10.1016/j.carbpol.2012.09.040

Tong, F., Deng, L., Sun, R., & Zhong, G. (2019). Effect of octenyl succinic anhydride starch ester by semi-dry method with vacuum-microwave assistant. *International Journal of Biological Macromolecules*, *141*, 1128-1136. https://doi.org/10.1016/j.ijbiomac.2019.08.157

Viana, E. B. M., Oliveira, N. L., Ribeiro, J. S., Almeida, M. F., Souza, C. C. E., Resende, J. V., Santos, L. S., & Veloso, C. M. (2022). Development of starch-based bioplastics of green plantain banana (*Musa paradisiaca* L.) modified with heat-moisture treatment (HMT). *Food Packaging and Shelf Life*, *31*, 100776. https://doi.org/10.1016/j.fpsl.2021.100776

Wang, H., Liu, Y., Chen, L., Li, X., Wang, J., & Xie, F. (2018). Insights into the multi-scale structure and digestibility of heat-moisture treated rice starch. *Food Chemistry*, *242*, 323-329. https://doi.org/10.1016/j.foodchem.2017.09.014

Wang, P. P., Luo, Z. G., Chun-Chen, Xiong-Fu, & Tamer, T. M. (2020). Effects of octenyl succinic anhydride groups distribution on the storage and shear stability of Pickering emulsions formulated by modified rice starch. *Carbohydrate Polymers*, *228*, 115389. https://doi.org/10.1016/j.carbpol.2019.115389

Wang, Q., Li, L., Liu, C., & Zheng, X. (2022). Heat-moisture modified blue wheat starch: Physicochemical properties modulated by its multi-scale structure. *Food Chemistry*, *386*, 132771. https://doi.org/10.1016/j.foodchem.2022.132771

Xie, X., Qi, L., Xu, C., Shen, Y., Wang, H., & Zhang, H. (2020). Understanding how the cooking methods affected structures and digestibility of native and heat-moisture treated rice starches. *Journal of Cereal Science*, *95*, 103085. https://doi.org/10.1016/j.jcs.2020.103085

Zainal Abiddin, N. F., Yusoff, A., & Ahmad, N. (2018). Effect of octenylsuccinylation on physicochemical, thermal, morphological and stability of octenyl succinic anhydride (OSA) modified sago starch. *Food Hydrocolloids*, *75*, 138-146. https://doi.org/10.1016/j.foodhyd.2017.09.003

Zavareze, E. D. R., & Dias, A. R. G. (2011). Impact of heat-moisture treatment and annealing in starches: A review. *Carbohydrate Polymers*, *83*(2), 317-328. https://doi.org/10.1016/j.carbpol.2010.08.064

Zhang, J., Ran, C., Jiang, X., & Dou, J. (2021). Impact of octenyl succinic anhydride (OSA) esterification on microstructure and physicochemical properties of sorghum starch. *LWT - Food Science and Technology*, *152*, 112320. https://doi.org/10.1016/j.lwt.2021.112320

Zhang, Z., Zhao, S., & Xiong, S. (2013). Molecular properties of octenyl succinic esters of mechanically activated Indica rice starch. *Starch/Starke*, *65*(5-6), 453-460. https://doi.org/10.1002/star.201200187

Zhou, J., Ren, L., Tong, J., & Ma, Y. (2009). Effect of Surface Esterification with Octenyl Succinic Anhydride on Hydrophilicity of Corn Starch Films. *Journal of Applied Polymer Science*, *114*(2), 940-947. https://doi.org/10.1002/app.30709